

Experimental Investigation of GFRP-Reinforced Hollow Square Concrete Column

Hussein Ali Hussein^{1,*}, AbdulMuttailb I. Said²

Department of Civil Engineering, College of Engineering, University of Baghdad, Baghdad, Iraq
hussein.hussein2001m@coeng.uobaghdad.edu.iq¹, dr.abdulmuttalib.i.said@coeng.uobaghdad.edu.iq²

ABSTRACT

Due to their great structural efficiency and efficient utilization of materials, steel-reinforced hollow-core concrete columns are often employed in utility poles, ground piles, and piers for bridges. Based on research, these columns' performance is impacted by many design parameters. However, corrosion can be a problem in steel-reinforced concrete structures. This paper examines the differences between using steel and GFRP longitudinal bars in hollow-section square concrete columns and explores the potential benefits of using GFRP bars as an option that is economically viable and non-corrosive. According to the study results, the computational results clearly show how an increased longitudinal GFRP reinforcement ratio improves the columns' bearing capability, but when compared to steel reinforcement, it provides less bearing capability. For the same reinforcement ratio (1.46 %, 3.29 %, and 4.9 %), The findings demonstrated that GFRP columns had a decrease in the axial bearing load by 13.1%, 9.2 %, and 9.4%, respectively.

Keywords: Hollow columns, Square section, Compression load, GFRP.

*Corresponding author

Peer review under the responsibility of University of Baghdad.

<https://doi.org/10.31026/j.eng.2024.06.07>

This is an open access article under the CC BY 4 license (<http://creativecommons.org/licenses/by/4.0/>).

Article received: 03/08/2023

Article accepted: 01/10/2023

Article published: 01/06/2024

دراسة تجريبية لعمود خرساني مربع مجوف مسلح بقضبان الياف الزجاج البوليمرية

حسين علي حسين^{*} ، عبد المطلب عيسى سعيد

قسم الهندسة المدنية، كلية الهندسة، جامعة بغداد، بغداد، العراق

الخلاصة

نظرًا لكفاءتها الهيكلية الكبيرة والاستخدام الفعال للمواد ، غالبًا ما يتم استخدام الأعمدة الخرسانية الأساسية المجوفة المسلحة بالحديد في أعمدة المرافق والأكوام الأرضية وأرصفتة الجسور. بناءً على البحوث ، يتأثر أداء هذه الأعمدة بالعديد من متغيرات التصميم. ومع ذلك ، يمكن أن يكون التآكل مشكلة في الهياكل الخرسانية المسلحة. تتضمن هذه الورقة البحثية الاختلافات بين استخدام قضبان التسليح الحديدية وقضبان الياف الزجاج البوليمرية في الأعمدة الخرسانية المربعة ذات المقطع المجوف وتكشف الفوائد المحتملة لاستخدام قضبان الياف الزجاج البوليمرية كخيار قابل للتطبيق اقتصاديًا وغير قابل للتآكل. وفقًا لنتائج الدراسة ، تُظهر النتائج الحسابية بوضوح كيف تعمل زيادة نسبة التسليح للقضبان الياف الزجاج البوليمرية الطولية على تحسين قدرة تحمل الأعمدة ، ولكن عند مقارنتها بتسليح الحديد ، فإنها توفر قدرة أقل على التحمل. لنفس نسبة التسليح (1.46% ، 3.29% ، 4.9%) أظهرت النتائج أن أعمدة الياف الزجاج البوليمرية لديها انخفاض في التحمل العمودي بنسبة 13.1% ، 9.2% ، و 9.4% على التوالي.

الكلمات المفتاحية: أعمدة مجوفة ، مقطع مربع ، حمل ضغط ، GFRP

1. INTRODUCTION

For axial loads to be transmitted inside a reinforced concrete structure, compression elements like columns, piles, and columns supporting bridge piers are crucial. These are crucial members, and if one fails in an important spot, the whole structure might collapse (Abbas and Awazli, 2017; Zakarea and Al-Baghdadi, 2020; Elmessalami et al., 2019). Hollow cores concrete columns are chosen over solid concrete columns for utility poles, ground piles, and the piers of high bridges because they have greater axial loads and bending moment resistance, greater structural effectiveness, a high strength-to-mass ratio, reduced self-weight, and more affordable styles (Ali et al., 2015; AL-Shaarbaf et al., 2017; Cassese et al., 2019; Abed and Alhafiz, 2019). These elements are often strengthened with steel bars, spirals, or ties. However, corrosion is becoming a major problem since hollow concrete columns have thinner walls and a smaller concrete cover for the steel reinforcing than solid concrete columns. It minimizes the axial loading capacity by damaging the steel bars of the transverse confinements.

As a result, there is growing interest in alternatives that aren't corrosive, like GFRP bars. According to (Rizkalla et al., 2003; El-Sallakawy et al., 2003; Benmokraune et al., 2006; Kim et al., 2014), and other researchers, GFRP bars have several benefits over steel, including reduced density, improved tensile strength, and resistance to corrosion even in hostile chemical conditions. While there has been significant research, despite the application of GFRP bars as flexural and shear reinforcements in concrete structures, the actual performance of GFRP-reinforced concrete compressive members is not yet fully understood. According to Standard ACI 440. R-06 (American Concrete Institute, 2006),



there is a need for further study in this area. Testing of GFRP bars under compressive load is complicated by the possibility of micro-buckling of fibers, due to the material's anisotropy and nonhomogeneity, and there is currently no accepted test method for compression load (Castro et al., 1995; Mirmiran et al., 2001; AlAjarmeh et al., 2019; Francis et al., 2010). The resistance of GFRP longitudinal reinforcement in compressive concrete components is not considered by American or the Canadian code (Canadian Standard Association, 2012). Research revealed that the compressive strength and modulus of (FRP) bars are lower than their tensile counterparts. Estimations suggest that the compression capacity of (GFRP) bars is approximately 55% of their tensile capacity. Investigations into GFRP bars with diameters of 15.9 mm, 19.1 mm, and 25.4 mm found that compressive strength often reached 77% of the tensile strength (Mander et al., 1983; Zahn et al., 1986; Malick et al., 1988; Mohamed and Benmokrane, 2014). In concrete prisms, GFRP bars subjected to compression forces at the center exhibited compressive strengths ranging from 30% to 40% of their tensile capacity. Axial load testing on 45 GFRP bars (15 mm in diameter, with unbraced lengths between 50 mm and 380 mm) revealed a compression capacity of approximately 50% relative to tensile capacity, with identical compressive and tension modulus (Chaallal and Benmokrane, 1993). Additionally, concrete beam columns (220 mm x 220 mm x 1850 mm) reinforced with GFRP were tested, showing that GFRP bars in compression members experienced strains of only 25% to 35% of their full strength (Zadeh and Nanni, 2013). Another study by (Deitz et al., 2003) examined small-scale square FRP-reinforced concrete columns (250 mm x 250 mm x 850 mm) using grid-type FRP for longitudinal reinforcement. Conservative estimates for axial load capacity were obtained by discounting GFRP bar participation. When replacing GFRP reinforcement with steel reinforcement in column specimens (400 mm x 200 mm x 1000 mm), the use of GFRP bars instead of longitudinal steel bars resulted in a 13% reduction in capacity (Paultre et al., 2010). However, switching steel ties to GFRP bars had only a 10% impact on strength, without affecting the load-deformation curve up to 80% of the ultimate load (Kobayashi and Fujisaki, 1995). Analytical investigations of short, thin reinforced concrete columns emphasized the importance of a minimum reinforcing ratio greater than 0.6% to prevent brittle failure (Alsayed et al., 1999).

Furthermore, considering GFRP reinforcement's contribution to compression zone strength is essential. GFRP-reinforced concrete columns exhibited behavior similar to steel-bar-reinforced columns, with GFRP and steel bar contributions to interior reinforcement strength estimated at approximately 5% and 16% of the ultimate capacity, respectively (De Luca et al., 2010). In conclusion, a study by (Tobbi et al., 2012) studied square-reinforced concrete columns with GFRP reinforcement, suggesting that the maximum load capacity could be approximated by assuming GFRP bar compressive capacity as 35% of the tensile strength. Despite these results, limited research has explored the functionality of GFRP-reinforced solid concrete columns, and the axial performance of GFRP hollow square concrete columns remains uninvestigated (Hoshikuma and Priestley, 2000; Carolin, 2003; Darwin et al., 2016; Liang and Sritharan, 2018; Hales et al., 2016; Raza and Ahmad, 2019).

This paper's goal was to study the investigation of the columns' compressive behavior on the square hollow-section concrete column reinforced with GFRP bar and the impact of longitudinal GFRP reinforcement ratio settings on their maximum load, failure, crack modes, and strain response. The study also compares the effects of the use of GFRP and steel as longitudinal reinforcements on structural behavior.



2. EXPERIMENTAL PROGRAM

In this work, six square hollow-section columns were created and tested by applying a compression load that was monotonically increased. They included three columns that were taken as references with steel bars and ties, and the other three columns with GFRP bars and steel ties. All test specimens had an exterior dimension of 180 x 180 mm, an interior hollow section measuring 70 x 70 mm, and a height of 900 mm. In this investigation, GFRP and steel reinforcement ratio was the primary experimental variable, in addition to reinforcement type (GFRP vs. steel).

2.1 Material Properties

The GFRP reinforcement had a deformed finish to improve the efficiency of the combination of the GFRP and concrete. All of the columns were reinforced using 12mm GFRP and steel bars to provide similar longitudinal reinforcement and 10mm steel stirrups as lateral reinforcement. According to the factory's datasheet, GFRP tensile properties are provided in **Table 1** for all hollow column specimens. The average compressive strength of the same day-cast column specimens made from ready-mixed concrete was 24.03 MPa. Compressive strength was determined by averaging the results of six 100 x 200 mm concrete cylinders tested on the same day as the column specimens.

Table 1. Properties of longitudinal and transverse reinforcement.

Material type	Diameter of bar (mm)	Elastic modulus (GPa)	Tensile strength (MPa)
GFRP	12	50	1200
Steel	12	200	530
Steel	10	200	525

2.2 Hollow Columns Specimen Preparation

The reinforcement information for the column specimens is shown in **Table 2**. Two codes are used to identify each specimen. Specimens that have steel or GFRP reinforcement are indicated by the letters **S** and **G**, respectively. The second part, which is the letters **R**, and the following number refers to the longitudinal steel or GFRP reinforcement ratio. Two categories were created from the specimens, as can be seen in **Fig. 1**. Group 1 includes three control specimens: the first column **SR1** with a reinforcement ratio of 1.46% by using 4 steel bars of 12 mm longitudinally, and the two other steel column specimens, **SR2** and **SR3**, which used 8 and 12 steel bars of 12 mm, respectively, achieved 3.29% and 4.9% longitudinal reinforcement ratios. 10 mm steel stirrups were used transversely with 170 mm spacing. Group 2 includes three specimens (**GR1**, **GR2**, and **GR3**) that were reinforced laterally with 10 mm steel ties with a constant spacing (170 mm). The same three longitudinal reinforcement ratios were handled, as illustrated in **Table 2**. The reinforcement ratios obtained using 4, 8, and 12 of 12 mm GFRP bars were 1.46%, 3.29%, and 4.9%, respectively. As can be seen in **Fig. 2**, a variety of column configurations were constructed using GFRP and

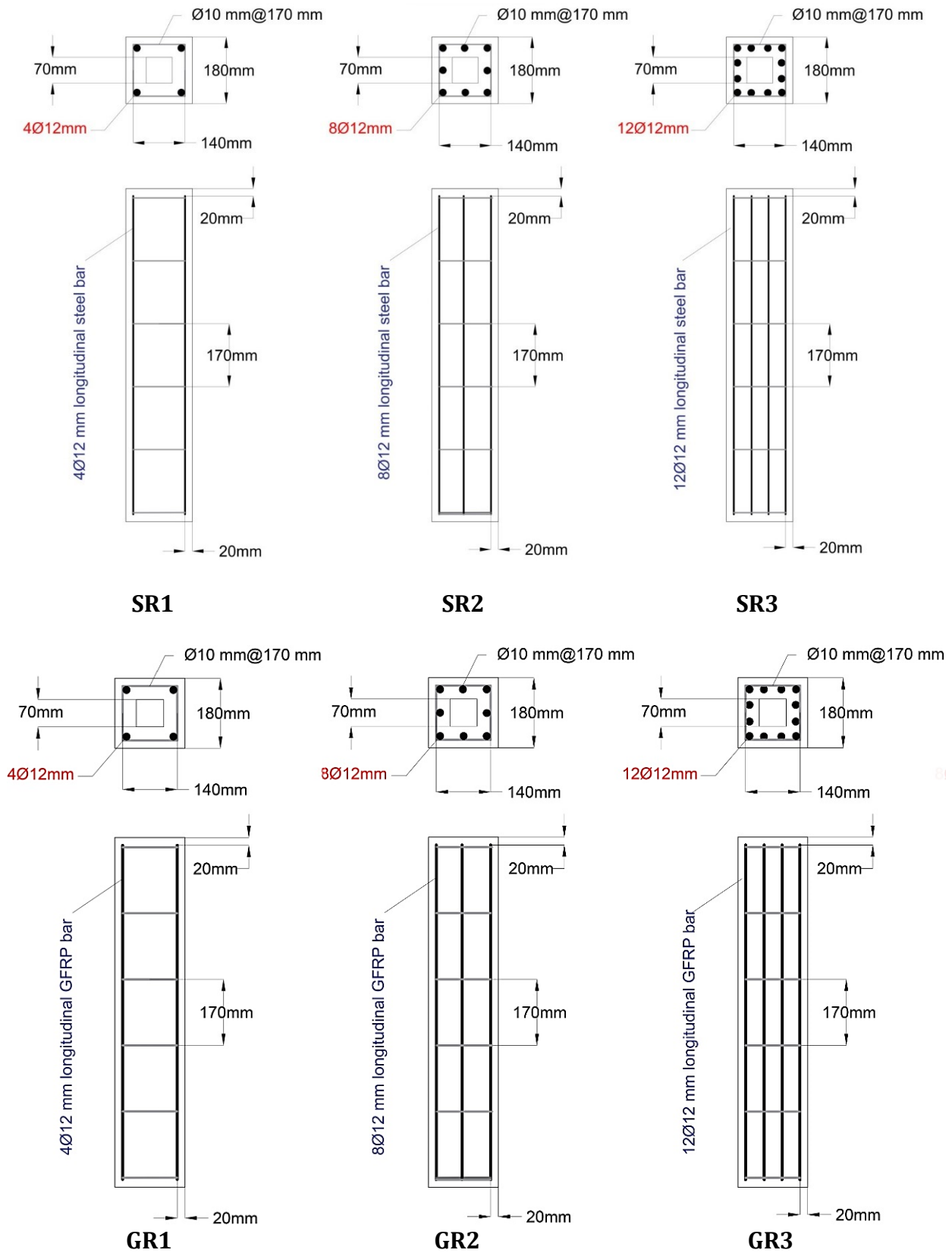


Figure 1. Structural details of Hollow square concrete column.

Table 2. Hollow square concrete column Specimen Details in this study.

Group no.	Specimens ID	Reinforcement type	Longitudinal reinforcement ratio %	Stirrups spacing (mm)	Hollow ratio
Group I	SR1	Steel	1.46	170	0.15
	SR2		3.29		
	SR3		4.9		
Group II	GR1	GFRP	1.46		
	GR2		3.29		
	GR3		4.9		



Figure 2. Reinforcement steel and GFRP cages.

steel cages. The distance between the concrete and the column sides was maintained at a constant 20 mm. As seen in **Fig. 3**, the square hollow columns were prepared to undergo horizontal casting in plywood molds. Then, the steel and GFRP reinforcements were put inside the plywood molds. As shown in **Fig. 4**, all columns were cast horizontally. A nearby ready-mix concrete supplier provided the concrete.



Figure 3. Details of hollow column plywood mold.



Figure 4. Casting concrete process.

2.3 Test Setup and Equipment

Column specimens were put to the test until they broke. Using the compression testing equipment at the University of Baghdad's Structural Laboratory under axial compressive stress with pinned end supports. The column specimen surface was cleaned and painted one day before testing. Under the column, a calibrated load cell with a 2000 kN capacity is used to calculate the total applied load. The total vertical displacement of the examined specimens was determined using LVDTs installed at the base of the machine that was used for testing, which moved up during the testing process. On the other hand, the horizontal displacement was measured using the two other LVDTs placed in the center of the specimens. Each column specimen has two square caps of steel 100 mm in height and 8 mm thick that were connected to the ends of the columns during the testing phase to prevent early collapse of the concrete in those areas owing to pressure intensity. Two strain gauges were used in each specimen; the first was attached at mid-height to measure and record the longitudinal strains, and the second was attached to the internal reinforcement at the longitudinal bar. The compressive loads and the resulting deformations were recorded throughout the testing period using an automated data-acquisition system. Fig. 5 presents the configuration and equipment utilized for this experimental research.

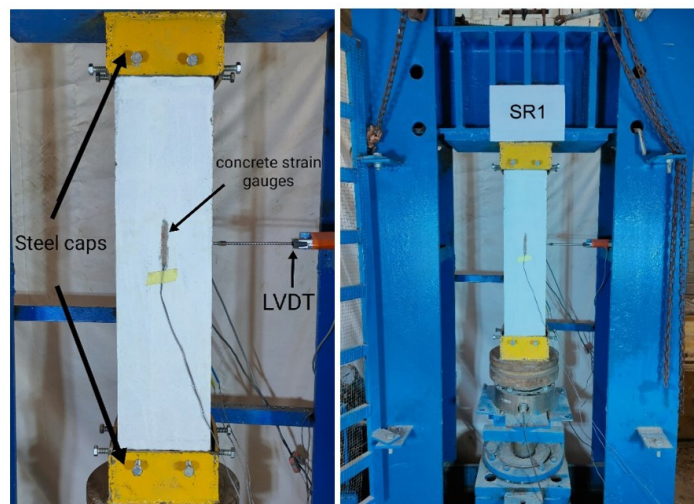


Figure 5. Compression machine and Test setup.



3. RESULTS AND DISCUSSION

Table 3. concludes the experiments of the studied columns. in terms of ultimate load (P_{ult}), axial displacement (Δ_{axial}), lateral displacement ($\Delta_{lateral}$), concrete strain ($\epsilon_{concrete}$), and strain in the longitudinal bar (ϵ_{bar}).

Table 3. Concrete Columns in the Present Study's Results.

Group no.	Column ID	Ultimate Load (KN)	Δ_{axial} (mm)	$\Delta_{lateral}$ (mm)	$\epsilon_{concrete}$ ($\mu\epsilon$)	ϵ_{bar} ($\mu\epsilon$)
Group 1	SR1	785.2	6.17	0.51	1701.1	2696.5
	SR2	1082.5	5.88	0.49	2107.6	2970.1
	SR3	1210.3	5.47	0.45	1980.7	2553.2
Group 2	GR1	682.6	5.54	0.47	1519.2	2913.9
	GR2	982.6	5.28	0.48	1938.6	2854.6
	GR3	1096.2	5.23	0.45	2280.9	3269.3

3.1 Crack Patterns and Failure Modes

Each column specimen was put to the test until it failed. Various failure modes were observed for the hollow concrete column, depending on the longitudinal and transverse reinforcing ratios and materials. Failure of GFRP longitudinally reinforced hollow columns often happened when the longitudinal bars ruptured (buckling or crushing), were explosive, and resulted in a complete loss of bearing capacity owing to consecutive longitudinal bar ruptures. The failure mechanism changed by longitudinally reinforcing the columns using steel bars as opposed to GFRP bars. Failure of column specimens reinforced longitudinally with steel bars was initiated by the observation of surface cracks in the specimens at about 65% of their ultimate capacity for the hollow columns. The concrete cover spalled as a result of further increases in the axial stress, which caused cracks to progressively spread at various locations on the specimens' faces. When the concrete cover began to spill, the core began to bear the load until the longitudinal bars buckled. For specimen **SR1**, the position of failure is located at the upper part of the test region, and for specimens **SR2**, and **SR3** the position of failure occurs near the middle height. Knowing that the failure distance decreases with increasing longitudinal reinforcement steel ratio. The reason for the failure is the excessive buckling of columns' longitudinal bars and a substantial decrease in load-bearing capacity induced by minor crushing of the core.

In all column specimens, there was no transverse reinforcement rupture failure. Failure in the GFRP longitudinally reinforced hollow columns showed nearly the same failure behavior and was sudden, more explosive, and relatively brittle than that of the hollow steel-reinforced columns. Limited vertical cracks began to show during testing at about 90% of the peak stresses on the columns. Before that, there were no visible fissures in the concrete cover. The cracks developed in the vertical direction enlarged and became bigger as the column stress increased until they reached the maximum load of the column. The GFRP columns showed a quick, explosive fracture and buckling without any transverse reinforcement rupture, and the concrete core was ultimately crushed. Each of the examined columns had a different mechanism and degree of longitudinal GFRP reinforcement rupture. According to the reinforcement ratio, group 2 specimens' inner concrete core damage levels varied; specimen **GR1** has Cracks that have propagated. The specimen's concrete cover

spalled at around mid-height, and the failure occurred due to all GFRP longitudinal bar rupture, which was reinforced with 4 bars of 12mm diameter with large damage in the concrete core. **GR2** also has cracking of the concrete overlaying the specimens' upper midsection, and the failure occurred due to all GFRP longitudinal bar rupture with massive damage in the concrete core. The GFRP longitudinal bar buckled and partially broke, causing **GR3** failure in addition to significant and loud cracking of the concrete core. All specimens' failure propagation is shown in **Fig. 6**.



Figure 6. Modes of failure for the tested specimens.

3.2 Effect of Variables on The Ultimate Load Capacity

3.2.1 Longitudinal Steel Reinforcement Ratio

Fig.7 clearly illustrates how longitudinal steel reinforcement affects the reinforced hollow square concrete's ability to bear loads. Three hollow column specimens of group 1 (**SR1**, **SR2**, and **SR3**) with reinforcement ratios of 1.46%, 3.29%, and 4.9%, respectively. As described previously, the specimen **SR1** shows an axial load capacity equal to 845.2kN. When increasing the longitudinal steel reinforcement ratios in the two other specimens (**SR2** and **SR3**), axial load capacities were 1082.5kN and 1210.3kN, respectively. There was an increase in the axial-bearing capacity by 28.07% and 43.1% concerning specimen **SR1**, and this increase is expected as a result of the increase in the area of the reinforcing steel and its participation in bearing the axial forces of the section.

3.2.2 Longitudinal GFRP Reinforcement Ratio

The reinforcement ratio had a significant impact on the behavior of the hollow concrete column that was reinforced with GFRP bars. The hollow concrete columns' ability to support an axial load improved when the reinforcement ratio increased. By comparing the ultimate load of group 2 column specimens (**GR1**, **GR2**, and **GR3**), the effect of the GFRP reinforcement ratio was determined. The concrete cross-section area of these columns was the same, but



they had various reinforcing ratios of (1.46%, 3.29%, and 4.9%), respectively. The first specimen **GR1** shows an axial load capacity equal to 682.6 KN, and for **GR2**, and **GR3**, the results showed an increase in axial load capacity of 43.9%, and 60.5%, respectively. **Fig. 8** shows the difference in load capacity between group 2 column specimens.

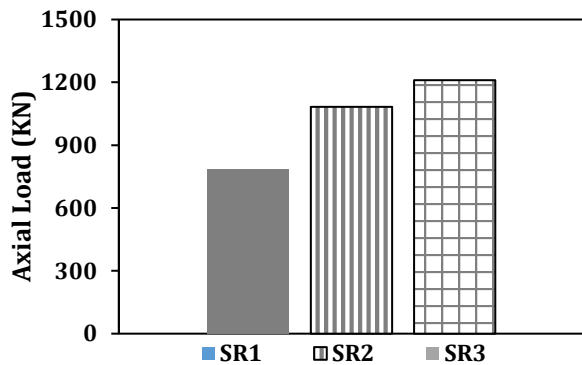


Figure 7. The effect of Longitudinal steel reinforcement ratio on total Load.

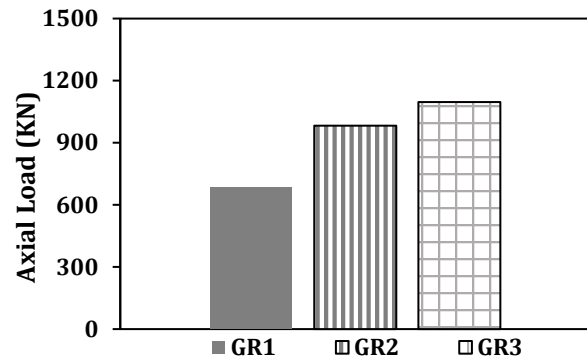


Figure 8. The effect of Longitudinal GFRP reinforcement ratio on total Load.

3.2.3 Longitudinal Reinforcement Type

Steel and glass fiber reinforced polymer (GFRP) mechanical characteristics are compared: steel is stiffer and exhibits elastic-plastic behavior before yielding, whereas GFRP is harder and exhibits linear elastic behavior up to failure. These differences may be seen in the material characteristics of the two kinds of bars. To find out the difference between hollow square concrete column specimens reinforced with steel and those reinforced with GFRP, a comparison was made between the specimens of group 1 and three other specimens of group 2, which have the same reinforcement ratio (1.46%, 3.29%, and 4.9%) but with a different type of longitudinal reinforcement, where GFRP bars were used in the specimens of group 2. The results showed that GFRP specimens (**GR1**, **GR2**, and **GR3**) had a decrease in the axial bearing load by 13.1%, 9.2%, and 9.4%, respectively, as shown in **Fig. 9**. This decrease in the ability to withstand compression loads is reasonable because the GFRP bars' elasticity is less than that of reinforcing steel bars (**Elchalakani et al., 2020**).

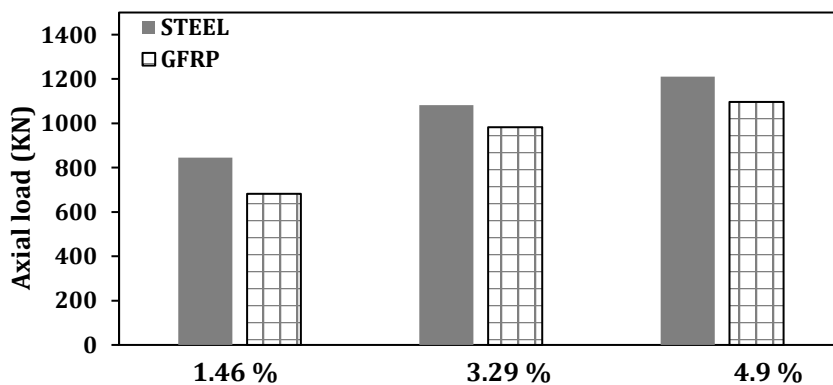


Figure 9. The effect of changing reinforcing type on the axial load capacity.

3.3 Load-Strain Relationship

The values of the strain in longitudinal reinforcement and concrete were calculated utilizing strain gages, as mentioned above. Curves of concrete strain versus load, longitudinal steel

bars, and GFRP bars were displayed and discussed in this part. When the load gradually increases, the strain begins to increase slightly in the elastic zone, with the onset of small cracks as the load increases until the column loads up to its full capacity. The descending curve of the relationship is not obtained due to a sudden failure of the column. For the first group, specimens **SR1**, **SR2**, and **SR3**, which have steel reinforcement, the results showed that the values of longitudinal steel strain were $2696 \mu\epsilon$, $2970 \mu\epsilon$, and $2553 \mu\epsilon$, respectively. These values represent the buckling failure in the longitudinal reinforcing steel. The value of axial concrete strain ranged between ($1701 \mu\epsilon$ to $2107 \mu\epsilon$) Noting that the model **SR2**, which has a longitudinal reinforcing ratio of 3.29 %, recorded the highest strain values for longitudinal steel bar and concrete. **Figs. 10 and 11** illustrate Load-steel and concrete strain curves for group 1 specimens.

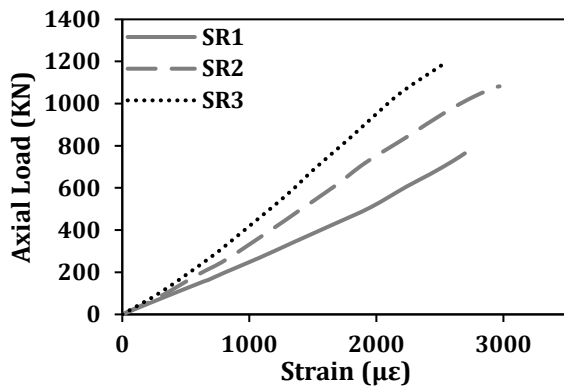


Figure 10. Load-steel strain response for group 1.

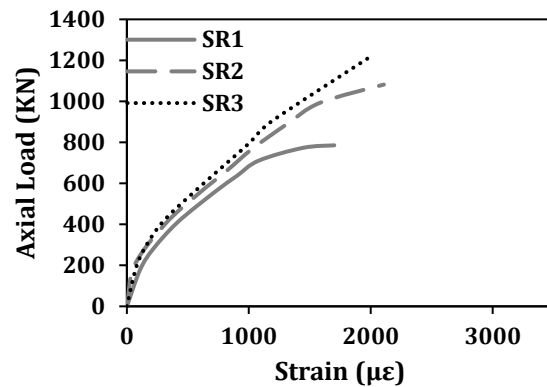


Figure 11. Load-concrete strain response for group 1.

The compression strain calculated in the GFRP longitudinal bars of group 2 specimens was approximately $3000 \mu\epsilon$, this is around 17.6% of the GFRP bars' maximum tensile strain. Columns **GR1** and **GR2** have measured strains of $2913 \mu\epsilon$ and $2854 \mu\epsilon$, respectively, whereas $3269 \mu\epsilon$ were in column **GR3**. and the concrete's vertical strain measurements varied from ($1519 \mu\epsilon$ to $2388 \mu\epsilon$), This is consistent with the level of strain at which cracks first appeared. The vertical strain readings began to lose accuracy after the hairline cracks began to appear. However, as can be seen in **Figs. 12 and 13**, this results in greater strains in GFRP bars. Referring to these figures, the maximum strain values were attained by the high reinforcement ratio GFRP bars.

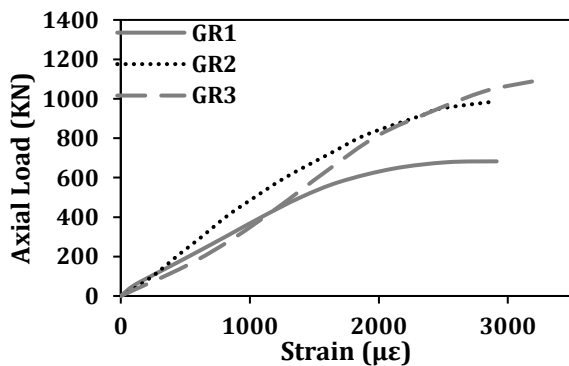


Figure 12. Load-steel strain response for group 2.

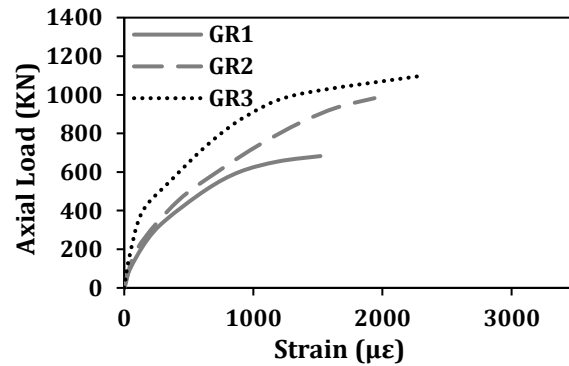


Figure 13. Load-concrete strain response for group 2.

3.4 Load-Displacement Relationship

The axial load-displacement response of steel-reinforced columns may be defined as a linear elastic ascending curve at the loading start. The longitudinal reinforcements and the whole part of the section's concrete were resisting the imposed load and deforming simultaneously up until the point at which they started to display nonlinear ascending behavior, which caused the column to exhibit a linear elastic behavior, which was about 65% of the ultimate applied load. The appearance of small cracks on the concrete's outside was the primary cause of nonlinear behavior up to the ultimate strength supported by the whole concrete area and the reinforcement running longitudinally before the outer concrete spalling in places. A considerable loss in load capacity because of the concrete cover falling apart. At this point, the column's gross area started to steadily decrease. and the steel bars continued to support the load and record strain while the contribution of the concrete was eliminated. Then the columns failed due to longitudinal steel bar buckling. For the first group, the model **SR1** showed an axial bearing capacity equal to 785.2 KN and an axial deformation of 6.17 mm. For the two other specimens (**SR2** and **SR3**), the test result showed axial bearing capacities of 1082.5 KN and 1210.3 KN, and there is a decrease in the axial displacement as the percentage of longitudinal reinforcement increases. The model **SR2** showed an axial displacement of 5.88 mm, and the model **SR3** showed an axial displacement of 5.47 mm. For the lateral displacement, almost close results were shown for the three specimens, ranging from (0.45 - 0.51) mm. The reason for the convergence of these values is that all the examined columns are short columns that have a small value of kl/r , in addition to that all the column specimens are loaded concentrically. Load-displacement responses for the specimens of group 1 are shown in **Figs. 14** and **15**.

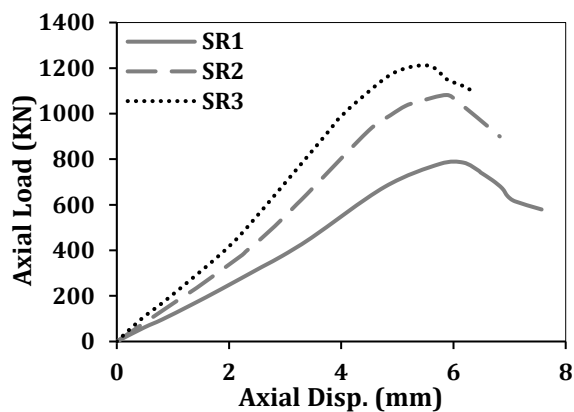


Figure 14. Load-axial displacement response for columns in group 1.

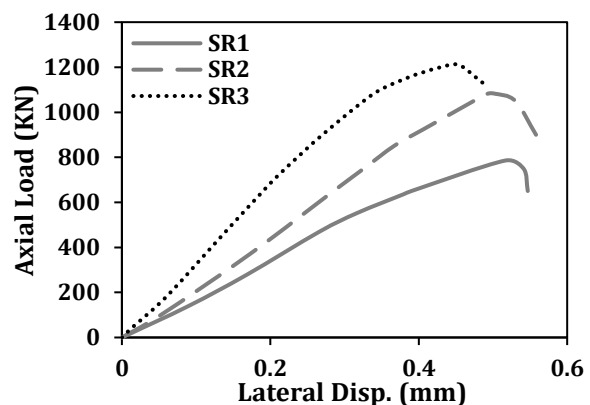


Figure 15. Load-axial displacement response for columns in group 1.

GFRP-reinforced columns exhibited load-displacement behavior that differed from that of the specimens with steel reinforcement. The columns showed stable loads and a linear-elastic part could not detect cracks in the concrete surface. Nonlinear behavior was, however, observed at approximately 90% of the ultimate applied load because hairline cracks began to spread just before the peak load capacity. The cover of the concrete was either totally or partly removed. Concrete spalling followed a large decrease in load brought on by the exploding concrete core. The GFRP longitudinal reinforcement then broke, leading to the ultimate column collapse at this point. According to the test findings, various axial-

load behaviors were recorded due to variable longitudinal GFRP bar features. For column specimens of group 2, **GR1** began with a straight upward slope. The crack propagation then caused a small nonlinear ascent leading up to the ultimate load of 682 kN at 5.54 mm. Columns **GR2**, and **GR3**, showed the same behavior but with a higher ultimate load capacity of 982 kN, and 1096 kN respectively, and as the longitudinal reinforcement ratio increases, the axial displacement decreases. So, the axial displacement of the specimens **GR2**, and **GR3**, was captured at 5.28 mm and 5.23 mm, respectively, at the moment of ultimate load. Load-displacement responses for the specimens of group 2 are shown in **Figs. 16 and 17**.

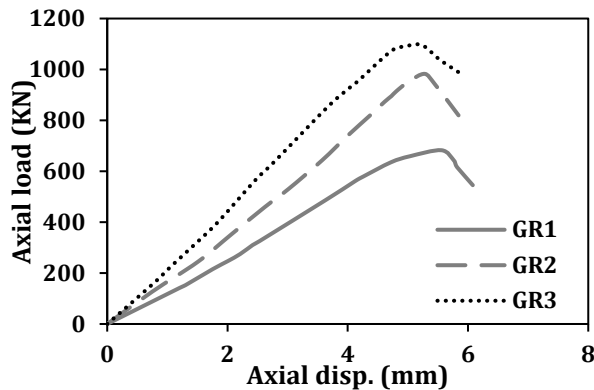


Figure 16. Load-axial displacement response for columns in group 2.

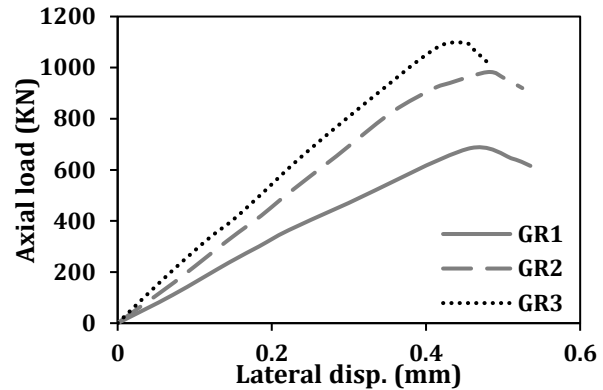


Figure 17. Load-axial displacement response for columns in group 2.

4. CONCLUSIONS

In this work, the behavior of a hollow square concrete column reinforced with GFRP bars was studied and compared with the behavior of steel-reinforced columns to expand knowledge and develop the possibility of using GFRP bars as internal reinforcement in columns due to the advantages it possesses. Based on the results obtained, several conclusions were noted, which can be summarized as follows:

- When the internal longitudinal reinforcement of hollow square GFRP column specimens was increased, the load-carrying capability also increased. By raising the reinforcement ratio from 1.46% to 3.29% and 4.9%, respectively, the axial load capacity was increased by 43.9% and 60.5% when compared to control columns.
- In contrast to steel-reinforced hollow column specimens and with the same reinforcement ratio (1.46%, 3.29%, and 4.9%), The findings revealed that GFRP specimens had a decrease in the axial bearing load by 13.1%, 9.2%, and 9.4%, respectively.
- The failure mechanism was changed by longitudinally reinforcing the columns with GFRP bars instead of steel bars. For GFRP longitudinally reinforced hollow columns, failure often happened after the longitudinal bars ruptured (buckling or crushing), and it was explosive with a complete loss of bearing capacity as a result of subsequent longitudinal bar ruptures. Failure of longitudinal steel bar columns was caused by excessive bar buckling without any rupture of the tie.
- The GFRP bars in the columns with high reinforcement ratios reached the highest strain values.
- It is suggested that switching steel reinforcement by GFRP bars reduces ductility.



NOMENCLATURE

Symbol	Description	Symbol	Description
A_{GFRP}	The gross cross-sectional area of the GFRP bar	LVDT	Linear Variable Differential Transducer
A_g	The gross cross-sectional area of the column	P_{bar}	Axial load capacity of the bar
A_{st}	Total area of longitudinal steel reinforcement	P_{cal}	Calculated compressive capacity
FRP	Fiber Reinforced Polymer	P_{ult}	Ultimate load capacity
f'_c	Compressive strength of concrete	P_{exp}	The compressive capacity results from the experiments
$f_{u,GFRP}$	The ultimate tensile strength of the GFRP bar	Δ_{axial}	Axial displacement
f_y	Steel yield strength	$\Delta_{lateral}$	Lateral displacement
GFRP	Carbon Fiber Reinforced Polymer	ϵ_{bar}	Strain in the longitudinal reinforcements
HCC	Hollow Concrete Columns	$\epsilon_{concrete}$	Corresponding concrete strain

Acknowledgments

The author is grateful for the academic support and resources provided by the Department of Civil Engineering, College of Engineering, University of Baghdad which significantly facilitated this study. This job could not have been completed without their assistance and contributions.

Credit Authorship Contribution Statement

Hussein Ali Hussein is responsible for collecting data, executing the experimental and numerical simulations, analyzing and interpreting the writing, and reviewing and editing the manuscript. AbdulMuttalib Issa Said supervised, reviewed, and edited the manuscript.

Declaration of Competing Interest

The authors declare that they have no known competing financial interests or personal relationships that could have appeared to influence the work reported in this paper.

REFERENCES

- Abbas, R.M., and Awazli, A.Q., 2017. Behavior of reinforced concrete column subjected to axial loads and cyclic lateral loading. *Journal of Engineering*, 23(2), pp. 23-42. [Doi:10.31026/j.eng.2017.02.03](https://doi.org/10.31026/j.eng.2017.02.03)
- Abed, F., and Alhafiz, A.R., 2019. Effect of basalt fibers on the flexural behavior of concrete beams reinforced with BFRP bars. *Composite Structures*, 215, pp. 23-34. [Doi:10.1016/j.compstruct.2019.02.050](https://doi.org/10.1016/j.compstruct.2019.02.050)
- ACI Committee, 2019. Building code requirements for structural concrete (ACI 318R-19) and commentary. American Concrete Institute, Farmington Hills, MI, pp. 623.



AlAjarmeh, O.S., Manalo, A.C., Benmokrane, B., Vijay, P.V., Ferdous, W. and Mendis, P., 2019. Novel testing and characterization of GFRP bars in compression. *Construction and Building Materials*, 225, pp. 1112-1126. [Doi:10.1016/j.conbuildmat.2019.07.280](https://doi.org/10.1016/j.conbuildmat.2019.07.280)

Ali, N.K., Salahldin, A. I., and Hamzaa, A. G., 2015. Impact analysis of reinforced concrete column with side opening subjected to eccentric axial load. *Journal of Engineering*, 21(2), pp. 1-29. [Doi:10.31026/j.eng.2015.02.01](https://doi.org/10.31026/j.eng.2015.02.01)

Alsayed, S.F., Al-Saloum, Y.A., Almusulam, G.H., and Amjjad, M.A., 1999. Concrete column reinforced by glass fiber reinforced polymers rod. *Special Publication*, 188, pp. 113-112. [Doi:10.14359/5614](https://doi.org/10.14359/5614)

AL-Shaarbaf, I.A., Allawi, A.A., and AlSallim, N.H. 2017. Strength of reinforced concrete column with transversal opening. *Journal of Engineering*, 23(10), pp. 124-143. [Doi:10.31026/j.eng.2017.10.09](https://doi.org/10.31026/j.eng.2017.10.09)

American Concrete Institute, 2006. *Guide for the designs and constructions of structure concrete reinforced with fiber-reinforced polymers (FRP) bar.(ACI 440.1 R-06)*. Farmington Hills, Michigan: American Concrete Institute.

Benmokraune, B., El-Sallakawy, E., El-Rageby, A., and El-Gamal, S., 2007. Performance evaluation of innovative concrete bridges deck slab reinforced with fibre-reinforced-polymers bar. *Canadian Journal of Civil Engineering*, 34(3), pp. 288-350. [Doi:10.1139/106-173](https://doi.org/10.1139/106-173)

Benmokraune, B., El-Sallakawy, E., El-Rageby, A., and Laclkey, T., 2006. Designing and testing of concrete bridges deck reinforced with glass FRPs bar. *Journal of Bridge Engineering*, 11(2), pp. 216-239. [Doi:10.1061/\(ASCE\)1084-0702\(2006\)11:2\(217\)](https://doi.org/10.1061/(ASCE)1084-0702(2006)11:2(217))

Canadian Standard Association, 2012. *Design and constructions of buildings component with fiber reinforced polymer*. CAN/ CSAS 806-12, Toronto.

Carolin, A., 2003. Carbon fiber reinforced polymers for strengthening of structural elements (Doctoral dissertation, Luleå tekniska universitet).

Cassese, P., De Risi, M.T., and Verderame, G.M., 2019. A degrading shear strength model for RC columns with hollow circular cross-section. *International Journal of Civil Engineering*, 17(8), pp. 1241-1259. [Doi:10.1007/s40999-018-0381-1](https://doi.org/10.1007/s40999-018-0381-1)

Castro, P.F., Howie, I., and Karbhari, V., 1995. Concrete columns reinforced with FRP rods. *International Journal of Materials and Product Technology*, 10(3-6), pp. 338-343. [Doi:10.1504/IJMPT.1995.036460](https://doi.org/10.1504/IJMPT.1995.036460)

Chaallal, O., and Benmokrane, B., 1993. Physical and mechanical performance of an innovative glass-fiber-reinforced plastic rods for concrete and grouted anchorages. *Canadian Journal of Civil Engineering*, 20(2), pp. 244-278. [Doi:10.1139/193-031](https://doi.org/10.1139/193-031)

Choo, C.C., Harrik, I.E., and Gesond, H., 2006. Strength of rectangular concrete column reinforced with fiber-reinforced polymers bar. *ACI Material Journal*, 113(3), p.542. [Doi:10.14359/15324](https://doi.org/10.14359/15324)

Darwin, D., Dolan, C.W., and Nilson, A.H., 2016. *Design of concrete structures (Vol. 2)*. New York, NY, USA, McGraw-Hill Education.

De Luca, A., Mata, F., and Nani, A., 2010. Behavior of full-scale glass fibers-reinforced polymers reinforced concrete column under axial loads. *ACI structural journal*, 107(5), P. 529. [Doi:10.14359/51663912](https://doi.org/10.14359/51663912)



- Deitz, D.H., Harik, I.E., and Gesund, H., 2003. Physical properties of glass fiber reinforced polymer rebar in compression. *Journal of Composite for Construction*, 7(4), pp. 333-346. [Doi:10.1061/\(ASCE\)1090-0268\(2003\)7:4\(363\)](https://doi.org/10.1061/(ASCE)1090-0268(2003)7:4(363))
- Elchalakani, M., Dong, M., Karrech, A., Mohamed Ali, M.S., and Huo, J.S., 2020. Circular concrete columns and beams reinforced with GFRP bars and spirals under axial, eccentric, and flexural loading. *Journal of Composites for Construction*, 24(3), P. 04020008. [Doi:10.1061/\(ASCE\)CC.1943-5614.0001008](https://doi.org/10.1061/(ASCE)CC.1943-5614.0001008)
- Elmessalami, N., El Refai, A., and Abed, F., 2019. Fiber-reinforced polymers bars for compression reinforcement: A promising alternative to steel bars. *Construction and Building Materials*, 209, pp. 725-737. [Doi:10.1016/j.conbuildmat.2019.03.105](https://doi.org/10.1016/j.conbuildmat.2019.03.105)
- El-Sallakawy, E., Benmokrane, B., and Desgagné, G., 2003. Fibre-reinforced polymers composites rebar for the concrete deck slabs of Woton Bridges. *Canadian Journal of Civil Engineerings*, 30(5), pp. 851-870. [Doi:10.1139/103-055](https://doi.org/10.1139/103-055)
- Francis, M., and Teng, B., 2010. Strength of short concrete columns reinforced with high modulus glass fibre reinforced polymer bars. In *Proceedings of the 2nd International Structures Specialty Conference*, pp. 45-1.
- Hales, T.A., Pantelides, C.P., and Reaveley, L.D., 2016. Experimental evaluation of slender high-strength concrete columns with GFRP and hybrid reinforcement. *Journal of Composites for Construction*, 20(6), P. 04016050. [Doi:10.1061/\(ASCE\)CC.1943-5614.0000709](https://doi.org/10.1061/(ASCE)CC.1943-5614.0000709)
- Hoshikuma, J.I., and Priestley, M.J.N., 2000. Flexural behavior of circular hollow columns with a single layer of reinforcement under seismic loading. *Ssrp*, 13.
- Kim, T.H., Lee, J.H., and Shin, H.M., 2014. Performance assessment of hollow RC bridge columns with triangular reinforcement details. *Magazine of Concrete Research*, 66(16), pp. 809-824. [Doi:10.1680/mac.13.00257](https://doi.org/10.1680/mac.13.00257)
- Kobayashi, K., and Fujisaki, T., 1995. 32 compressive behaviour of FRPs reinforcements in non-prestressed concrete member. In *Non-Metallic (FRP) Reinforcement for Concrete Structure: Proceedings of the Second International RILEM Symposium* (Vol. 29, p. 367). CRC Press.
- Liang, X., and Sritharan, S., 2018. Effects of confinement in circular hollow concrete columns. *Journal of Structural Engineering*, 144(9), P.04018159. [Doi:10.1061/\(ASCE\)ST.1943-541X.0002151](https://doi.org/10.1061/(ASCE)ST.1943-541X.0002151)
- Lotfy, E.M., 2010. Behavior of reinforced concrete short columns with Fiber Reinforced polymers bars. *International Journal of Civil and Structural Engineering*, 1(3), P. 545.
- Malick, P.K., 1988. *Fiber reinforced composites, materials, manufacturing, and design*, Marcel Dekker, New York. [Doi:10.1080/10426918908956295](https://doi.org/10.1080/10426918908956295)
- Mander, J.B., Priestley, M.J.N., and Park, R., 1983. Behavior of ductile hollow reinforced concrete columns. *Bulletin of the New Zealand Society for Earthquake Engineering*, 16(4), pp. 273-290. [Doi:10.5459/bnzsee.16.4.273-290](https://doi.org/10.5459/bnzsee.16.4.273-290)
- Mirmiran, A., Yuan, W., and Chen, X., 2001. Design for slenderness in concrete columns internally reinforced with fiber-reinforced polymer bars. *Structural Journal*, 98(1), pp. 116-125. [Doi:10.14359/10153](https://doi.org/10.14359/10153)



- Mohamed, H.M., and Benmokrane, B., 2014. Design and performance of reinforced concrete water chlorination tank totally reinforced with GFRP bars: Case study. *Journal of Composites for Construction*, 18(1), P. 05013001. [Doi:10.1061/\(ASCE\)CC.1943-5614.0000429](https://doi.org/10.1061/(ASCE)CC.1943-5614.0000429)
- Paultre, P., Eid, R., Langlois, Y., and Lévesque, Y., 2010. Behavior of steel fiber-reinforced high-strength concrete columns under uniaxial compression. *Journal of Structural Engineering*, 136(10), pp. 1225-1235. [Doi:10.1061/\(ASCE\)ST.1943-541X.0000211](https://doi.org/10.1061/(ASCE)ST.1943-541X.0000211)
- Raza, A., and Ahmad, A., 2019. Numerical investigation of load-carrying capacity of GFRP-reinforced rectangular concrete members using CDP model in ABAQUS. *Advances in Civil Engineering*, 2019. [Doi:10.1155/2019/1745341](https://doi.org/10.1155/2019/1745341)
- Rizkalla, S., Hasan, T., and Hasan, N., 2003. Design recommendation for the usage of FRPs for reinforcement and strengthening of concrete structure. *Progress in Structural Engineering and Material*, 6(1), pp. 18-28. [Doi:10.1002/pse.139](https://doi.org/10.1002/pse.139)
- Tobbi, H., Farghally, A.S., and Benmokrane, B., 2012. Concrete column reinforcement longitudinally and transversally with glass fiber-reinforced polymers bar. *ACI Structural Journal*, 108(6). pp. 551-558.
- Zadeh, H.J., and Nanni, A., 2013. Design of RC columns using glass FRP reinforcement. *Journal of Composites for Construction*, 17(3), pp. 294-304. [Doi:10.1061/\(ASCE\)CC.1943-5614.0000354](https://doi.org/10.1061/(ASCE)CC.1943-5614.0000354)
- Zahn, F.A., Park, R. and Priestley, M.J.N., 1986. *Design of reinforced bridge columns for strength and ductility*. Rep. 86, 7.
- Zakarea, A.W. and Al-Baghdadi, H.B., 2020. Experimental and numerical study on CFRP confinement square concrete compressive member subjected to compression load. *Journal of Engineering*, 26(4), pp. 142-180. [Doi:10.31026/j.eng.2020.04.10](https://doi.org/10.31026/j.eng.2020.04.10)